RSC Advances

PAPER

View Article Online
View Journal | View Issue

Cite this: *RSC Adv.*, 2021, **11**, 29042

Fabrication and characterization of structurally stable pH-responsive polymeric vesicles by polymerization-induced self-assembly

Fen Zhang, *[a] Yanling Niu,[b] Yantao Li, [a] Qian Yao,[a] Xiaoqi Chen,[a] Haijun Zhou,[a] Mengmeng Zhou[a] and Jijun Xiao*[b]

Received 20th July 2021
Accepted 16th August 2021

DOI: 10.1039/d1ra05555k

rsc.li/rsc-advances

Smart polymeric vesicles with both tertiary amine and epoxy functional groups were fabricated for the first time *via* a reversible addition–fragmentation chain transfer dispersion polymerization approach, using (2-(diisopropylamino)ethyl methacrylate (DIPEMA) and glycidyl methacrylate (GlyMA) in an ethanol–water mixture. Monitoring of the *in situ* polymerization revealed the low molecular weight distributions and the intermediate structures of spheres and worms, indicating an evolution in particle morphology. A phase diagram was constructed for reproducible fabrication of the vesicles, and copolymer composition was found to be more related to particle morphology. The vesicles exhibited superior structural stability for the cross-linking of the core through epoxydiamine chemistry, and intelligent pH responsibility due to the presence of the tertiary amine groups. The cross-linked vesicles showed good stability and reversibility during the swelling and shrinking cycles by switching the pH values, which endowed them with potential cell-like transmission functions. This research thus provides a method for producing structurally stable pH-responsive polymeric vesicles, and the reported vesicles are based on commercially available starting materials for possible industrial scale-up.

Introduction

Nanoparticles have attracted significant attention due to their broad applications in areas of catalysis, drug delivery, imaging, and sensing.[1–5] Self-assembly of block copolymers is the most common method for preparing block copolymer nanoparticles with a diverse set of morphologies. However, this method is normally conducted in highly diluted solutions (typically less than 1% solid content) *via* post-polymerization processing steps, and it is difficult to implement on a large scale.[6–9] Polymerization-induced self-assembly (PISA) is a recently developed one-pot polymerization approach that can generate multiple morphologies such as micelles, as well as worm-like/rod-like and spherical vesicles at high yields and with high solid content (typically 10–50 wt%).[10–13]

Compared to other polymer nanoparticles, polymeric vesicles have attracted more attention due to their internal and external hydrophilic properties, and hydrophobic membrane core, which makes them useful for medical applications such as hydrophobic and hydrophilic medical carriers. Reversible addition–fragmentation chain transfer (RAFT)-mediated dispersion polymerization is the most commonly used PISA strategy for preparing polymeric vesicles. In this method, the monomer is dissolved/miscible in the solvent, but the polymer is not. During polymerization, a hydrophilic macromolecular chain transfer agent (macro-CTA) is chain extended with a second or third monomer to form an insoluble block segment. Once the amphiphilic block copolymer reaches a certain degree of polymerization, it starts self-assembling to form nanoparticles, and polymerization continues within the nanoparticles.[14,15]

Structural stability is important for polymeric vesicles, to prevent disassembly due to dilution, external stimuli such as changes in pH or oxidation/reduction, or the addition of a solvent for both blocks.[16–18] To increase the mechanical stability and options for membrane permeability, cross-linking within the membrane core or the hydrophilic corona has become a viable option. Several research groups have investigated covalent cross-linking *via* either *in situ* cross-linking through copolymerization with a divinyl comonomer or post polymerization chemical reactions. For *in situ* cross-linking, if the cross-linker is added at the beginning of polymerization, it will reduce the chain mobility of the produced block copolymers and thus hinder morphology transition into vesicles. Cross-linked vesicles with a symmetric divinyl comonomer have been reported by the Armes group,[19,20] where a divinyl comonomer such as ethylene glycol dimethacrylate (EGDMA) was added after consumption of the core-forming monomer. This

[a]*Institute of Energy Resources, Hebei Academy of Sciences, 050081, Shijiazhuang, Hebei Province, China. E-mail: fen.zhang1105@hotmail.com*

[b]*School of Materials Science and Engineering, Hebei University of Science and Technology, 050018, Shijiazhuang, Hebei Province, China. E-mail: jijunxiao@aliyun.com*

prevented the cross-linker on the vesicle from forming a highly cross-linked third block. Alternatively, An *et al.*[21] developed an *in situ* cross-linking strategy to stabilize vesicles using an asymmetric cross-linker such as allylacrylamide (ALAM), which was added prior to the commencement of polymerization. Because of the limitations of *in situ* cross-linking, either two-step feeding or special monomers and cross-linkers are needed; the post polymerization chemical reactions are more designable for polymeric vesicles. Post polymerization chemical cross-linking can be used to form shell-cross-linked vesicles, as described by Sumerlin *et al.*,[22] along with core-cross-linked vesicles, which have been reported by various studies.[19,23–26]

Along with polymeric vesicles, the incorporation of stimulus-responsive characteristics such as pH, temperature, oxidation/reduction, and light within the polymeric vesicles have become a possibility for controlling the capture and release of drugs and chemicals.[2,14,27] Compared with other external properties, the applications of pH-responsive nanoparticles for controlled release/encapsulation are of interest for a wide range of pH gradients in biological and physiological systems.[28] In general, pH-responsive nanocarriers can be fabricated from polymers with acid-labile functional groups like β-carboxylic amides, acetal, orthoester, hydrazone, and oxime bonds, and boronic acid esters.[29–32] Additionally, switching between hydrophilic (swollen) and hydrophobic (collapsed) states results in the protonation and deprotonation of functional groups, such as amine and carboxylic acid groups, in response to changes in environmental pH.[33] This later method does not generate any small toxic molecules and is therefore generally used to produce pH-responsive nanocarriers.

Thus, polymeric vesicles with stable structures and pH responsibility may potentially be used for biomedical applications. Recently, smart polymeric vesicles with cross-linked cores were produced by using two functional monomers, (2-(diisopropylamino)ethyl methacrylate (DIPEMA) and 7-(2-methacryloyloxy-ethoxy)-4-methylcoumarin (CMA)), with a macro-RAFT agent poly(*N*-(2-hydroxypropyl) methacrylamide) (PHPMA). After vesicle formation, UV irradiation was used to initiate the cross-linking of the CMA units, and the produced vesicles exhibited pH-responsive permeability.[34] However, the CMA comonomer is not commercially available and needs to be custom made. Glycidyl methacrylate (GlyMA), which is a commodity monomer, has been widely used for coatings, catalysis, biomedical analysis, biomolecular separation, and gene delivery.[35–37] The epoxy moiety can be functionalized with alcohols, thiols, amines, or proteins. In addition, epoxydiamine chemistry is an easy way to achieve covalent cross-linking, as studied by Armes,[16] Tan,[26] and Chen[38] *et al.*

To the best of our knowledge, there have been almost no reports on the synthesis of polymeric vesicles with both tertiary amine and epoxy functional groups. Zhu *et al.*[39] used *N*,*N*-dimethylaminoethyl methacrylate (DMAEMA) and GlyMA to prepare a functional copolymer PDMAEMA-*co*-PGlyMA with 2-cyanoprop-2-yldithionaphthalate (CPDN) as a RAFT agent and *N*,*N*′-azobis(isobutyronitrile) (AIBN) as the initiator for bulk polymerization. However, only a well-defined PDMAEMA-*co*-PGlyMA copolymer with tertiary amine and epoxy functional groups was synthesized. Herein, we report the copolymerization of DIPEMA and GlyMA with poly(ethylene oxide)-4-(4-cyanopentanoic acid) dithiobenzoate (mPEG-CPADB) as the macro-chain-transfer agent in an ethanol/water solvent for the preparation of polymeric vesicles. We also further cross-linked the obtained polymeric vesicles by using ethylenediamine to produce structurally stable pH-responsive vesicles (Scheme 1). PEG was selected to produce the macro-chain-transfer agent in this study, due to its effective steric stabilization, high biocompatibility, and low immunogenicity, and there have been a number of FDA-approved PEGylated therapeutic entities.[40–42] The fabrication of the vesicles *via* RAFT dispersion copolymerization of DIPEMA and GlyMA, as well as the cross-linking of the vesicles and pH responsibility, were studied in detail. In addition, the monitoring of *in situ* polymerization by transmission electron microscopy (TEM) revealed intermediate spheres and worm structures, indicating an evolution in particle morphology. The produced cross-linked vesicles exhibited good morphology in the dimethyl sulfoxide (DMSO) solvent, disassembly of the non-cross-linked structures, and the cross-linked vesicles showed good stability and reversibility during the swelling and shrinking cycles by switching between pH values of 4.0 and 8.0. This endowed the materials with potential cell-like transmission functions.

Experimental section

Materials

The α-methoxy-ω-hydroxypoly(ethylene oxide) (mPEG) with a number average molecular weight (M_n) of 1900 was purchased from Aladdin and used as received. The 4-(4-cyanopentanoic acid) dithiobenzoate (CPADB), 4-(dimethylamino)pyridine, and dicyclohexylcarbodiimide compounds were purchased from Aladdin and also used as received. Additionally, 2-(diisopropylamino)-ethyl methacrylate (DIPEMA, Aladdin, 97%) and glycidyl methacrylate (GlyMA, Aladdin) were purified by passing the compounds through a column of Al_2O_3 to remove the inhibitor prior to use. Lastly, *N*,*N*′-azobis(isobutyronitrile) (AIBN, Tianjin Chemical Reagent Co. Ltd) was purified *via* recrystallization from ethanol. All other chemicals were of analytical grade and used without further purification.

Synthesis of the macro-RAFT agent (mPEG-CPADB)

Synthesis of the macro-RAFT agent, mPEG-CPADB, was conducted according to the methods described in the literature.[26,43] A solution of mPEG (1.9000 g, 1.0000 mmol), CPADB (0.8370 g, 3.0000 mmol), and 4-(dimethylamino)pyridine (0.0366 g, 0.4000 mmol) in 30 ml of anhydrous dichloromethane was added into a 100 ml round-bottom flask. Then, dicyclohexylcarbodiimide (0.6180 g, 3.0000 mmol) was dissolved in 5 ml of anhydrous dichloromethane, which was added dropwise into the above solution contained in an ice bath. After dicyclohexylcarbodiimide was completely added, the esterification reaction proceeded under stirring at room temperature for three days. Then, the opaque solution was filtered to remove the *N*,*N*′-dicyclohexylurea. The polymer was collected by precipitation in

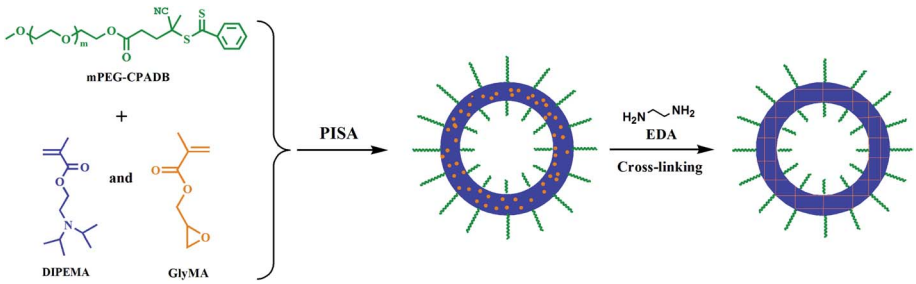

Scheme 1 Fabrication of pH-responsive vesicles by PISA and epoxydiamine chemistry for the core cross-linking of the vesicles.

ice diethyl ether three times, and a pink powder was obtained after drying under vacuum conditions overnight.

RAFT dispersion copolymerization of DIPEMA and GlyMA

A typical protocol for the RAFT dispersion polymerization with a total solid concentration of 15% was performed, according to the following methods. First, DIPEMA (0.2730 g, 1.2800 mmol), GlyMA (0.0455 g, 0.3200 mmol), mPEG-CPADB (0.0440 g, 0.0200 mmol), AIBN (0.0011 g, 0.0067 mmol), and a solvent (2.0700 g, with a mass ratio of ethanol/water = 6 : 4) were added into a glass tube with a magnetic bar. This reaction mixture was degassed *via* N_2 purge in an ice bath for 30 min. After degassing by three pump-N_2 purge cycles, the glass tube was sealed under a vacuum. The sealed tube was placed in an oven at 70 °C under magnetic stirring, and the polymerization was performed for 7 h. The reaction mixture was quickly cooled to room temperature and then opened to air to quench the polymerization. The reaction temperature, ethanol/water ratio, macro-RAFT agent/initiator ratio used in the polymerization were all optimized as above for getting polymeric vesicles with tertiary amine and epoxy functional groups.

Cross-linking of the produced vesicles

A typical protocol for the covalent cross-linking of the mPEG-P(DIPEMA-*co*-GlyMA) vesicles with 15 wt% solid content was as follows. First, 0.2000 g of the produced mPEG-P(DIPEMA-*co*-GlyMA) vesicles with 15 wt% solid content were diluted 20-fold with ethanol/water (6 : 4 weight ratio), and ethylenediamine (0.0016 g, 0.0266 mmol, ethylenediamine/GlyMA molar ratio = 1 : 1) was added to the aqueous dispersion mixture. The epoxy-amine reaction then proceeded under stirring for 24 h at room temperature. The samples were purified *via* centrifugation–redispersion cycles to remove excess ethylenediamine.

Characterization

The ^{1}H NMR (500 MHz) spectra were obtained using a Bruker DMX500 spectrometer, where $CDCl_3$ was used as the solvent and tetra-methylsilane was used as an internal reference. A Waters 2695 gel permeation chromatograph (GPC) equipped with an RI 410 detector was used to measure the molecular weight (M_n) and molecular weight distribution (M_w/M_n). THF was used as the eluent with a flow rate of 1.0 ml min^{-1}, and monodispersed polystyrene standards were used for the calibration of molecular weight and M_w/M_n. The samples for the GPC test were isolated by freeze-drying and then solved in THF for testing. The morphologies of the nano-objects were characterized with transmission electron microscopy (TEM), which was performed on a JEM-2100Plus electron microscope at an accelerating voltage of 200 kV. The samples for TEM observations were prepared by depositing the produced nano-object dispersions in ethanol/water on copper grids, which were successively coated with thin carbon films. Then, the sample was stained with phosphotungstic acid before observations were made. The conversion of the reaction mixture was calculated by weighing. All of the dynamic light scattering measurements were carried out on a commercial dynamic light scattering (DLS) spectrometer (PPS Z3000, Particle Sizing Systems, UK) equipped with an He–Ne laser (15.0 mW, 635 nm) at 25 °C and a fixed angle of 90°, and all the data were averaged over three measurements. The Fourier transform infrared (FTIR) spectroscopy was obtained using a PerkinElmer Frontier and was employed to characterize the reaction between ethylene diamine and the epoxy groups.

Results and discussion

Synthesis of macro-CAT agent mPEG-CPADB

Synthesis of the macro-CAT agent mPEG-CPADB was conducted according to the methods described in the literature,[26,43] and mPEG with a molecular weight (M_n) of 1900 was used for the esterification reaction with CPADB to produce the macro-CAT agent, mPEG-CPADB. Excess CPADB was used in this reaction to ensure high end-functionality, and the residual CPADB was removed by precipitation in cold diethyl ether. As shown in Fig. 1(a), the GPC result (M_w/M_n) of mPEG was 1.15, and mPEG-CPADB macro-CTA with M_w/M_n = 1.18 was prepared. The ^{1}H NMR spectroscopy results (Fig. 1(b)) indicated high end-functionality (>97%) based on the integral signal values of the methoxy protons for PEG at δ = 3.4 (h) and the aromatic protons at δ = 7.3–8.0 (a, b, c). These results were similar to the results found in the literature.[43]

Fabrication of vesicles *via* RAFT dispersion copolymerization of DIPEMA and GlyMA

DIPEMA, which has been widely for fabricating pH-responsive nano-objects due to its adjustable pH-induced water solubility,[34,43–45] was selected to fabricate the vesicles with pH-

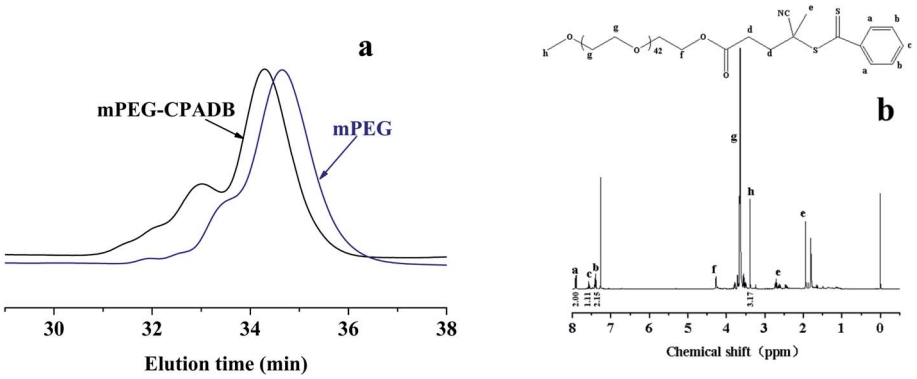

Fig. 1 GPC spectrum of mPEG and mPEG-CPADB with THF as the eluent (a), and the ^{1}H NMR spectrum of mPEG-CPADB in $CDCl_3$ (b).

regulated permeability during RAFT dispersion polymerization. GlyMA, which has reactive epoxy groups, was used to copolymerize with DIPEMA to produce vesicles with both tertiary amine and epoxy functional groups. In dispersion polymerization, the solvent is an important parameter, and its effect on the reaction is complicated. This method also requires all of the components to dissolve in the reaction mixture, however the formed polymer has poor solubility in the solvent. Thus, DIPEMA and PDIPEMA are soluble in ethanol and immiscible in water, while GlyMA is ethanol soluble and PGlyMA is immiscible in both ethanol and water. Consequently, a mixture of ethanol and water was selected as the reaction solvent for the

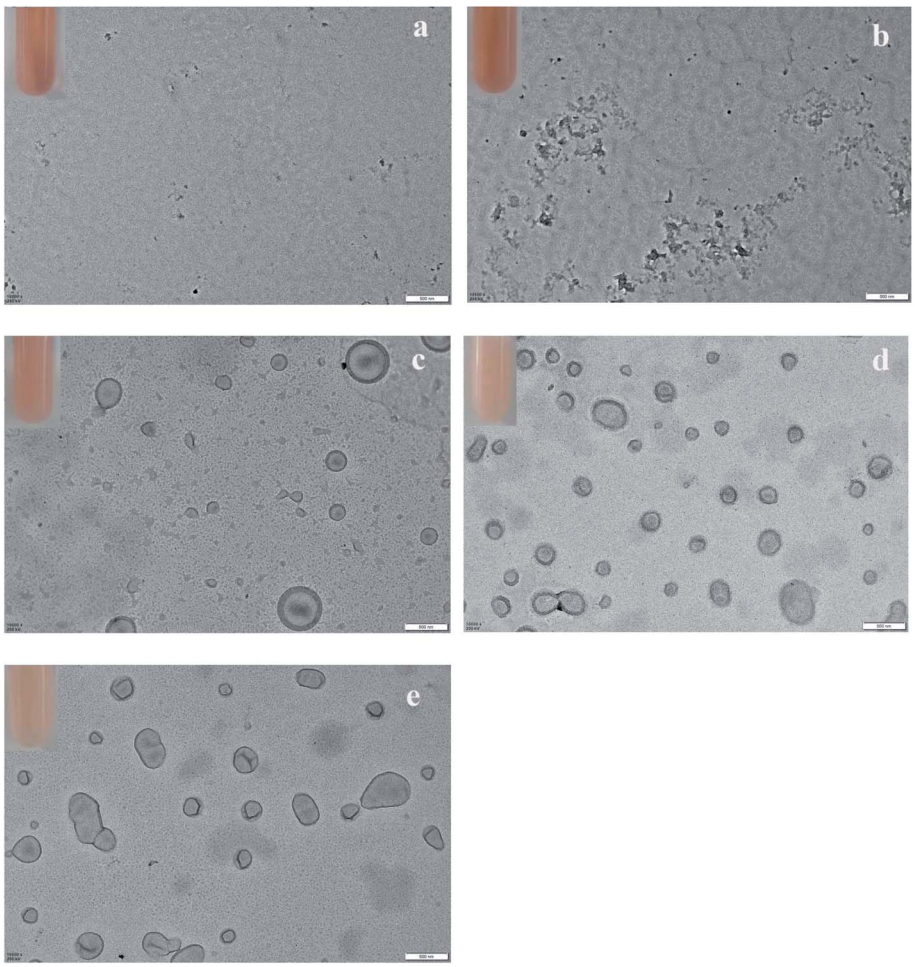

Fig. 2 TEM micrographs and photographs of the produced product in a reaction medium of ethanol/water, with varying amounts of water: (a) 10, (b) 20, (c) 30, (d) 40, and (e) 50 wt%. The other reaction parameters were: DIPEMA/GlyMA molar ratio = 8 : 2, mPEG-CPADB/AIBN molar ratio = 3 : 1, solid content 10 wt%, and reaction time = 7 h.

Table 1 Effects of water content on the conversion of the reaction mixture

Water content[a]/wt%	Conversion/%
10	70.42
20	75.59
30	85.17
40	92.77
50	98.59

[a] wt% relative to the solvent content. The other reaction parameters were: DIPEMA/GlyMA molar ratio = 8 : 2, mPEG-CPADB/AIBN molar ratio = 3 : 1, solid content 10 wt%, reaction time = 7 h.

copolymerization of DIPEMA and GlyMA, and the effects of the ethanol/water ratio on the produced nanoparticles were studied.

During the investigation, we found that up to 50 wt% of water in the reaction medium could be added to maintain a homogeneous reaction mixture before polymerization. Fig. 2 shows the particle morphology and photographs of the reaction mixture. Table 1 also lists the effects of water content on the conversion of the reaction mixture, corresponding to Fig. 2. As shown in Fig. 2, when a high amount of ethanol content was used (ethanol/water weight ratio = 9 : 1 & 8 : 2) as the solvent, a translucent reaction mixture was obtained (photographs in Fig. 2(a) & (b)), and only the polymer film and irregular particles were observed in the TEM figures. When the water content was increased to 30 wt%, well-shaped vesicles were found (Fig. 2(c)), and polymers that did not form particles could still be observed. After further increasing the water content, the reaction mixture became more turbid after the reaction finished, as shown in the photographs in Fig. 2(d) & (e), and only polymeric vesicles were observed in the TEM photos. As detailed in Table 1, the water content seriously affected the conversion, with 70.42% in the 10 wt% water system and 98.59% in the 50 wt% water system at fixed mPEG-CPADB/AIBN content, solid content, polymerization time, and temperature. It is commonly known that substantially higher conversion and faster polymerization rates can be expected for alcoholic RAFT PISA formulations with higher water content.[26,46–48] Thus, water is a nonsolvent for the growing core-forming P(DIPEMA-*co*-GlyMA) block, leading to particle nucleation at a shorter critical degree of polymerization (DP). Both DIPEMA and GlyMA have relatively low solubility in water, therefore the addition of water to the continuous phase should encourage more monomers into the particle phase for polymerization. However, in the low water reaction system, for good solubility of PDIPEMA in ethanol, only smaller parts of the polymer chains with PGlyMA blocks and higher molecular weights could precipitate out to form nuclei. Furthermore, homogeneous solution polymerization promoted chain radical termination, which prevented P(DIPEMA-*co*-GlyMA) polymer molecular weight growth, and most stayed in the continuous phase, which affected the eventual yield. Therefore, the water co-solvent played an important role at the molecular level in the PISA polymerization system, which was conducted in the alcohol/water mixtures.

Kinetics studies of the RAFT dispersion copolymerizations of DIPEMA and GlyMA were conducted in a 40 wt% water system with a target degree of polymerization (DP) of 80 for the core-forming block, with a solid content of 10 wt%. Five reactions with same formulation were done in parallel, and the polymerization process was followed by stopping the reaction at various reaction times. Subsequently, each sample was characterized by its conversion, number average molecular weight, particle morphology, and particle diameter. The results are presented in Fig. 3 and 4, where Fig. 3 shows the evolution of the conversion, particle diameter, number average molecular weight, and molecular weight distributions *versus* polymerization time, while Fig. 4 illustrates the TEM images at various polymerization times.

When the reaction proceeded for 120 min, the conversion rate was 46%, the reaction mixture was still transparent, and black dots with polymer film were visible in the TEM photo, as shown in Fig. 4(a). When the reaction proceeded for 140 min, a light turbid reaction mixture was observed, which indicated the onset of nucleation. The conversion increased to 52.6%, and mixtures of vesicles, worms, non-spherical vesicles, and tiny dots were observed, as shown in Fig. 4(b). The DLS result showed that the particle diameter increased from 116 nm at

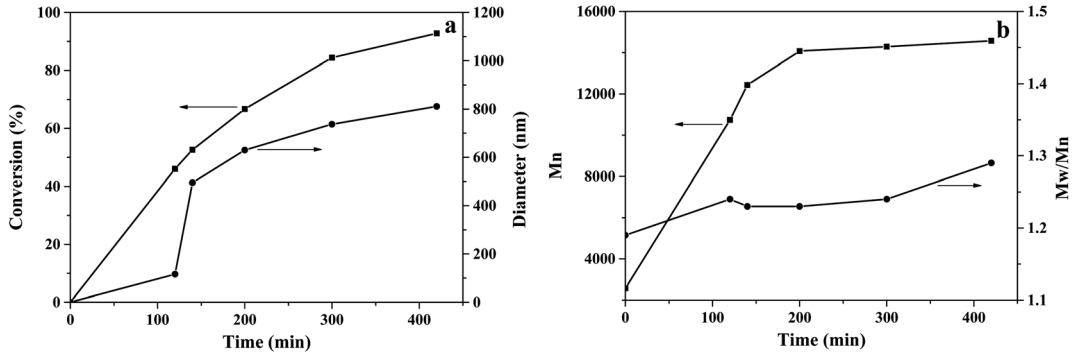

Fig. 3 (a) Conversion evolution and particle diameter *versus* polymerization time, and (b) the number average molecular weight and molecular weight distribution *versus* polymerization time in an ethanol–water mixture with 40 wt% of water. The other reaction parameters were: DIPEMA/GlyMA molar ratio = 8 : 2, mPEG-CPADB/AIBN molar ratio = 3 : 1, solid content 10 wt%.

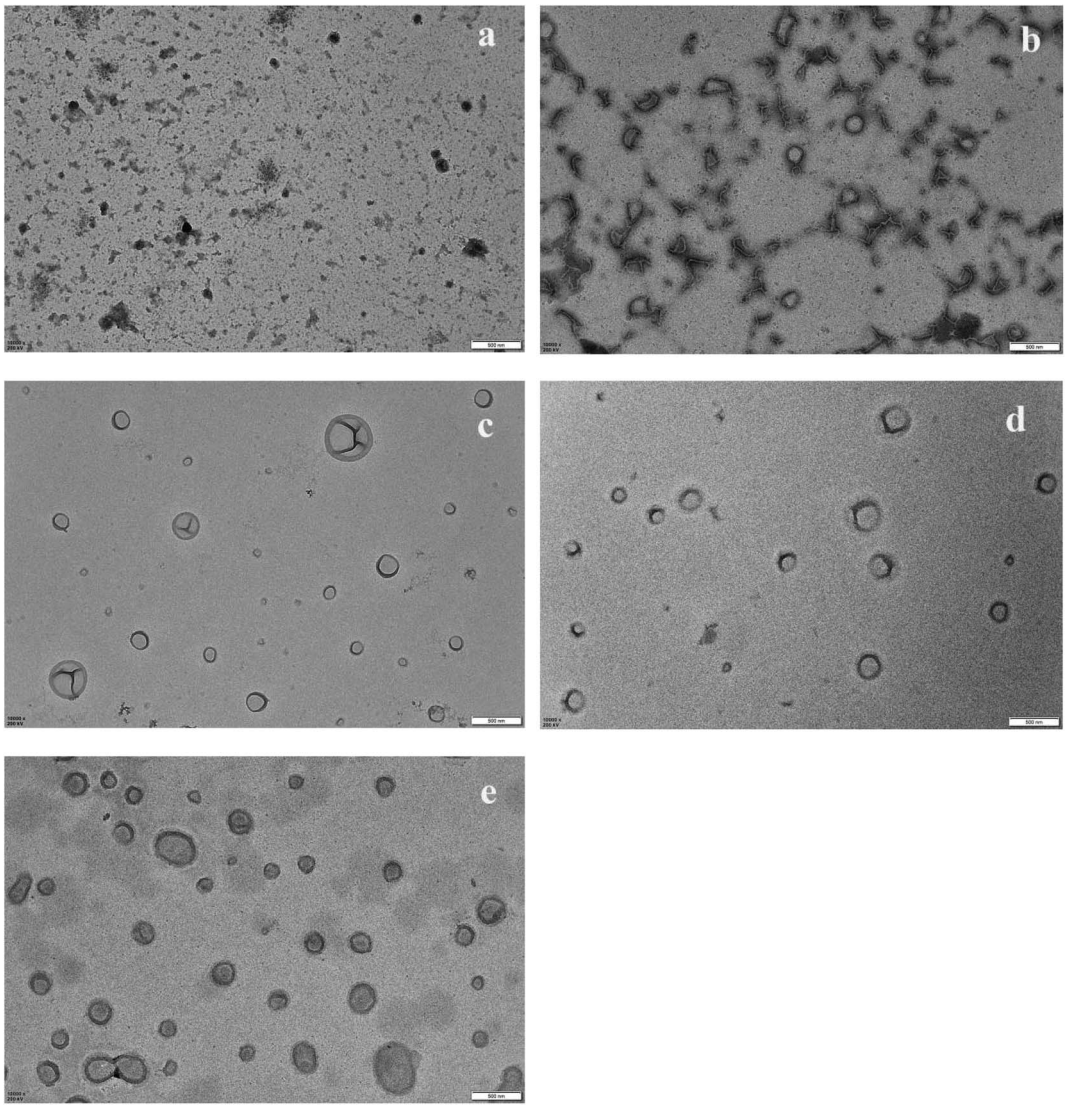

Fig. 4 TEM images obtained at various reaction times in the ethanol–water mixture containing 40 wt% of water. The other reaction parameters were: DIPEMA/GlyMA molar ratio = 8 : 2, mPEG-CPADB/AIBN molar ratio = 3 : 1, solid content 10 wt%, (a) 120 min, (b) 140 min, (c) 200 min, (d) 300 min, and (e) 420 min.

120 min of reaction time to 495 nm after 140 min, based on the calculation model of the DLS machine, which indicated fast aggregation of the unstable particles. The reaction was allowed to continue, and when the reaction proceeded for 200 min, the tiny dots disappeared and well-shaped vesicles with large and small sizes were observed, with an average vesicle diameter of about 630 nm.

Subsequently, the vesicles grew larger by either growing internally and/or aggregating. The thickness of the vesicle membrane increased and aggregation continued after the reaction proceeded for 300 min, as shown in Fig. 4(e), and vesicles with long spherical shapes were observed. The above observations were consistent with the studies of the Armes' group,[15] which found an evolution in the particle morphology from sphere-to-worm-to-vesicle transitions for 2-hydroxypropyl methacrylate (HPMA) polymerization with poly(glycerol monomethacrylate) (PGlyMA). The chain transfer agent was in an aqueous solution, while the onset of nucleation was longer (~140 min *vs.* ~60 min) for the present polymerization system because of the good solubility of PDIPEMA in ethanol and the inefficient packing of PGlyMA chains at high temperatures, which increased the critical length of the precipitation chains. The molecular weight curve showed similar trends for conversion. For the first 200 min during the reaction, the conversion increased quickly, and the M_n also showed a sharp increase. After the reaction proceeded for 300 min, the conversion was higher than 80% and the M_n increased very slowly. Low molecular weight distributions were also observed throughout polymerization, as shown in Fig. 3(b), and the M_w/M_n values were around 1.23 after a shorter reaction time, and increased to 1.29 at about 93% monomer conversion, showing molecular weight distributions similar to Tan's report for the RAFT

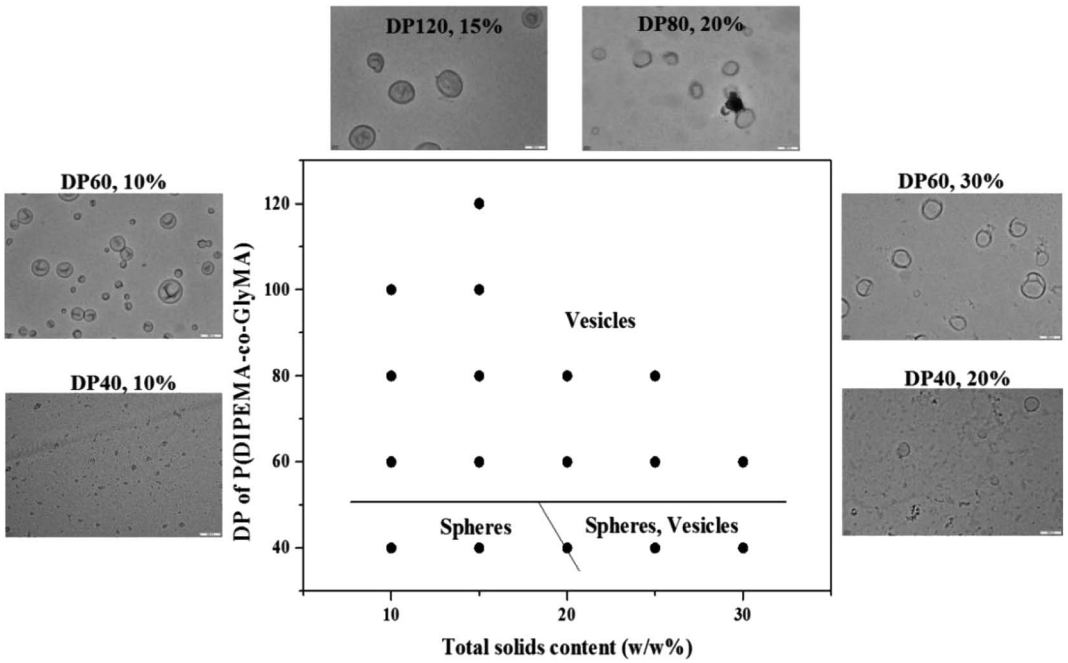

Fig. 5 Phase diagram for mPEG-P(DIPEMA-*co*-GlyMA) at 70 °C by varying the target DP of P(DIPEMA-*co*-GlyMA) and the solid content. Phase regions consisted of spheres and vesicles.

dispersion polymerization of GlyMA *via* photo-initiation in an ethanol–water solvent.[26]

A series of RAFT dispersion copolymerizations of DIPEMA and GlyMA were conducted by varying the solid content and the DP of the P(DIPEMA-*co*-GlyMA) block, to prepare various morphologies for the construction of a phase diagram, as shown in Fig. 5. This was helpful for the reproducible fabrication of morphological nano-particles. A mixed solvent containing ethanol/water = 6 : 4 (weight ratio) and a feed molar ratio of DIPEMA/GlyMA = 8 : 2 was used in this study. Fig. 5 shows that the polymeric vesicles formed in a large space, and only spheres and vesicles were obtained with solid content between 10 to 30% in this polymerization system, after the polymerization proceeded for 7 h and the DP of the core-forming block P(DIPEMA-*co*-GlyMA) was more associated with particle morphology. When the target DP of P(DIPEMA-*co*-GlyMA) was equal to or higher than 60, pure vesicles were obtained with a solids content of 10–30%. Additionally, pure solid particles were produced when the target DP of P(DIPEMA-*co*-GlyMA) was equal to or lower than 40 with a solids content of less than 20%, along with solid particles and vesicle mixtures with solid content higher than 20%. Based on previous reports,[10,34,49,50] other than solid content, copolymer composition significantly influenced the final morphologies. The morphology of the copolymer prepared *via* PISA was determined primarily by the relative volume fractions of the constituent blocks (packing parameter, P, $P = v/(al)$, where v is the volume of the hydrophobic polymer chain, a is the optimal interfacial area per molecule and l is the hydrophobic length normal to the interface). Thus, spherical particles were expected when P was $\leq 1/3$, while worms and vesicles were expected for $1/3 \leq P \leq 1/2$ and $1/2 \leq P \leq 1$, respectively.[28,51,52] The good solubility of PDIPEMA in ethanol and the inefficient packing of the PGlyMA chains at 70 °C increased the critical length of the precipitation chains and the volume of the hydrophobic polymer chain was larger. Thus the vesicles could be formed at a lower target DP, compared to other RAFT aqueous or alcoholic dispersion polymerization systems, where DP is generally equal or higher than 80 for methacrylate monomers to obtain vesicles.[12,15,16,26,34,43]

Cross-linking of the vesicles

The mPEG-P(DIPEMA-*co*-GlyMA) vesicles prepared in this study contained epoxy functionality in their cores, and further cross-linking was conducted to enhance the stability of the vesicles and avoid typical disassembly of the polymer membrane upon application of the pH stimulus or solvent. The mPEG-P(DIPEMA-*co*-GlyMA) vesicles (prepared at 15 wt% solid content with a feed molar ratio of DIPEMA/GlyMA = 8 : 2) were treated with ethylenediamine (EDA) in an ethanol/water mixture (weight ratio 60 : 40) at room temperature for 24 h (EDA/GlyMA molar ratio = 1 : 1). The samples were then purified *via* centrifugation–redispersion cycles to remove excess EDA.

The chemical structure of the mPEG-P(DIPEMA-*co*-GlyMA) vesicles before reaction with EDA was characterized by ^{1}H NMR, and Fig. 6(a) shows the ^{1}H NMR analysis result. The peaks at δ 3.2 (e), δ 2.63 and 2.82 (f) can be assigned to the protons of the epoxy group, and δ 4.23 and 3.84 (d) were attributed to –OCH_2– protons of PGlyMA units (the two protons labeled d were in different chemical environments and consequently gave two different resonances), while δ 3.84 (a) attributed to –OCH_2– protons of PDIPEMA units. The molar composition of PGlyMA and PDIPEMA in the copolymer is 19.3% and 80.7% respectively

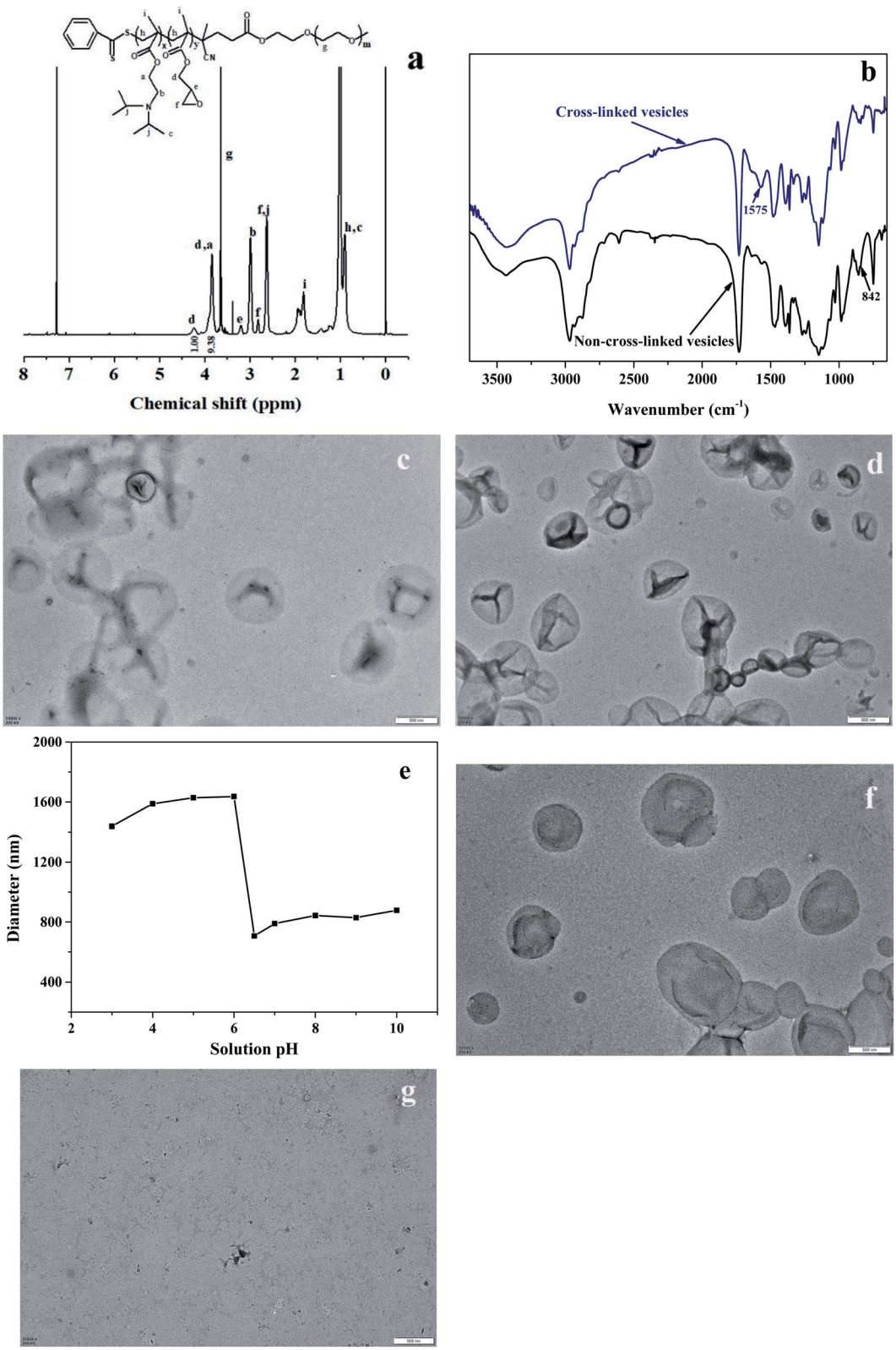

Fig. 6 (a) ^{1}H NMR spectra of mPEG-P(DIPEMA-*co*-GlyMA) vesicles, (b) FTIR spectra of mPEG-P(DIPEMA-*co*-GlyMA) vesicles before and after reacting with EDA, (c) TEM image of cross-linked mPEG-P(DIPEMA-*co*-GlyMA) vesicles after dispersing in the ethanol/water mixture, (d) TEM image of cross-linked mPEG-P(DIPEMA-*co*-GlyMA) vesicles after dispersing in DMSO, (e) diameter of cross-linked mPEG-P(DIPEMA-*co*-GlyMA) vesicles *vs.* pH variation, (f) TEM image of cross-linked mPEG-P(DIPEMA-*co*-GlyMA) vesicles in acidic solution (pH 6.0), (g) TEM image of non-cross-linked mPEG-P(DIPEMA-*co*-GlyMA) vesicles in acidic solution (pH 6.0).

by calculation based on the integral area of the peak a and peak d. The cross-linking of the vesicles was conducted by reacting the epoxy groups with EDA. Fourier transform infrared (FTIR) spectroscopy was employed to characterize the reaction between EDA and the epoxy groups, and Fig. 6(b) shows the FTIR spectra of the mPEG-P(DIPEMA-*co*-GlyMA) vesicles before and after cross-linking. The absorption peak at 842 cm^{-1} (from the epoxy group) became smaller after the reaction, which confirmed the conversion of the epoxy groups. The absorption peak at 1575 cm^{-1} (from the primary amine group) also indicated the reaction of the EDA with the epoxy groups. To verify that the mPEG-P(DIPEMA-*co*-GlyMA) vesicles were indeed cross-linked after reacting with EDA, the purified samples were dispersed in a dimethyl sulfoxide (DMSO) solvent, which is a good solvent for mPEG, PDIPEMA, and PGlyMA. Vesicle morphology was then observed by TEM. Fig. 6(c) shows the morphology of the vesicles after dispersion in the ethanol/water mixture, while Fig. 6(d) shows the TEM image of the vesicles after dispersion in DMSO. The images show that the morphologies of vesicles were well maintained, indicating that the vesicles were cross-linked after reacting with EDA.

Due to deprotonation and protonation of the tertiary amine groups in PDIPEMA (pK_a is around 6.3), the polymer chains transformed from a hydrophobic state at a high pH value to a hydrophilic state at low pH. The variations in hydrodynamic diameter of the cross-linked vesicles *versus* pH values of the solution were studied, as shown in Fig. 6(e). When the solution pH was higher than 6.50, the vesicles obtained after EDA treatment had similar diameters (around 800 nm, Fig. 6(e)) because of their unprotonated hydrophobic states. Due to protonation of the tertiary amine groups in the P(DIPEMA-*co*-GlyMA) chains at a low pH, for example below 6.0 pH, the diameter of the cross-linked vesicles expanded to around 1600 nm. This occurred because the cross-linked P(DIPEMA-*co*-GlyMA) chains of the vesicle walls became hydrophilic and the vesicles were highly swollen, while the non-cross-linked vesicles dispersed in the ethanol/water solution became transparent when the pH was adjusted to less than or equal to 6.0. Fig. 6(f) shows the morphology of the cross-linked vesicles at a pH of 6.0, and Fig. 6(g) shows the non-cross-linked vesicles. Well-shaped vesicles are shown in Fig. 6(f), while only polymer film is visible in Fig. 6(g), which further illustrated that cross-linking of the vesicle membrane endowed the vesicles with superior structural stability.

To verify the stability and reversibility of the cross-linked vesicles during the swelling and shrinking cycles, diameter changes were studied by switching the pH of the solution between a pH of 8.0 and 4.0. Fig. 7 shows the results of the five cycles. The pH value of the above solution was adjusted by adding an NaOH aqueous solution (0.1 M) and an HCl aqueous solution (0.1 M). At a pH of 8.0, the PDIPEMA block was deprotonated and hydrophobic, and vesicles with a diameter of around 800 nm were observed. In an acidic solution (pH = 4.0), the PDIPEMA block was protonated and hydrophilic, and the vesicles were swollen but did not disassemble and had a diameter of around 1600 nm. The diameter of the cross-linked mPEG-P(DIPEMA-*co*-GlyMA) vesicles showed no obvious changes after five swelling–shrinking cycles, indicating that the cross-linked structure was very stable.

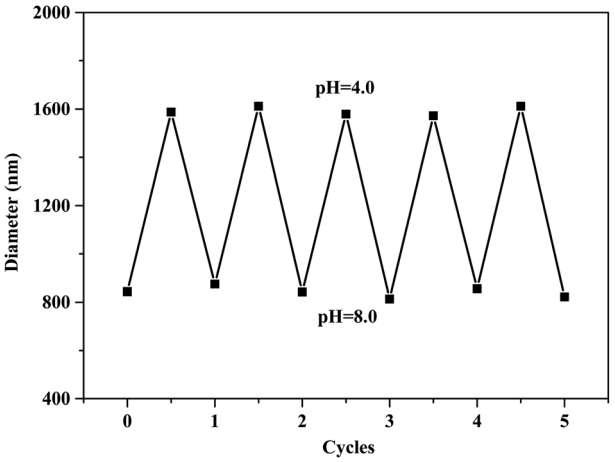

Fig. 7 Reversible diameter changes of the vesicles between a pH of 4.0 and 8.0.

Conclusions

In summary, the smart vesicles developed in this study exhibited superior structural stability due to the cross-linking of the core through epoxydiamine chemistry. The vesicles also displayed intelligent pH responsibility for the existing tertiary amine groups, which endowed the vesicles with potentially cell-like transmission functions. The effect of water content in the solvent was one of the key factors for vesicle formation, and when the DP of the P(DIPEMA-*co*-GlyMA) copolymer was equal to or higher than 60, it produced stable mPEG-P(DIPEMA-*co*-GlyMA) vesicles. The selected starting materials are commercially available, and the utilized RAFT dispersion polymerization method is reliable for industrial scale-up. Given the efficiency of RAFT dispersion polymerization and scalability, the pH responsible, cross-linked vesicles produced by this method could potentially be used for drug release and nanoreactors.

Author contributions

The manuscript was written with contributions of all authors. All authors have given approval to the final version of the manuscript.

Conflicts of interest

There are no conflicts to declare.

Acknowledgements

We gratefully acknowledge the financial support from the Hebei Academy of Sciences (21703), and thank LetPub (http://www.letpub.com) for its linguistic assistance during the preparation of this manuscript.

Notes and references

1 A. Lu, T. P. Smart, T. H. Epps, D. A. Longbottom and R. K. O'Reilly, *Macromolecules*, 2011, **44**, 7233–7241.
2 X. L. Hu, Y. Q. Zhang, Z. G. Xie, X. B. Jing, A. Bellotti and Z. Gu, *Biomacromolecules*, 2017, **18**, 649–673.
3 Q. M. Liu, H. S. Zhu, J. Y. Qin, H. Q. Dong and J. Z. Du, *Biomacromolecules*, 2014, **15**, 1586–1592.
4 L. Qiu, C. R. Xu, F. Zhong, C. Y. Hong and C. Y. Pang, *ACS Appl. Mater. Interfaces*, 2016, **8**, 18347–18359.
5 Z. F. Huang, Y. L. Chen, R. Z. Wang, C. Y. Zhou, X. B. Liu, L. C. Mao, J. Y. Yuan, L. Tao and Y. Wei, *RSC Adv.*, 2020, **10**, 5704–5711.
6 R. C. Hayward and D. J. Pochan, *Macromolecules*, 2010, **43**, 3577–3584.
7 Y. Y. Mai and A. Eisenberg, *Chem. Soc. Rev.*, 2012, **41**, 5969–5985.
8 Y. Wang, C. Y. Hong and C. Y. Pan, *Biomacromolecules*, 2013, **14**, 1444–1451.
9 C. Gao, Y. Wang, W. P. Zhu and Z. Q. Shen, *Chin. J. Polym. Sci.*, 2014, **32**, 1431–1441.
10 N. J. Warren and S. P. Armes, *J. Am. Chem. Soc.*, 2014, **136**, 10174–10185.
11 J. T. Sun, C. Y. Hong and C. Y. Pan, *Polym. Chem.*, 2013, **4**, 873–881.
12 N. J. W. Penfold, J. R. Whatley and S. P. Armes, *Macromolecules*, 2019, **52**, 1653–1662.
13 C. Gonzato, M. Semsarilar, E. R. Jones, F. Li, G. J. P. Krooshof, P. Wyman, O. O. Mykhaylyk, R. Tuinier and S. P. Armes, *J. Am. Chem. Soc.*, 2014, **136**, 11100–11106.
14 W. J. Zhang, C. Y. Hong and C. Y. Pan, *Macromol. Rapid Commun.*, 2018, **40**, 1800279.
15 A. Blanazs, J. Madsen, G. Battaglia, A. J. Ryan and S. P. Armes, *J. Am. Chem. Soc.*, 2011, **133**, 16581–16587.
16 P. Chambon, A. Blanazs, G. Battaglia and S. P. Armes, *Langmuir*, 2012, **28**, 1196–1205.
17 S. Moreno, B. Voit and J. Gaitzsch, *Colloid Polym. Sci.*, 2021, **299**, 309–324.
18 J. Gaitzsch, D. Appelhans, L. Wang, G. Battaglia and B. Voit, *Angew. Chem., Int. Ed.*, 2012, **51**, 4448–4451.
19 K. L. Thompson, P. Chambon, R. Verber and S. P. Armes, *J. Am. Chem. Soc.*, 2012, **134**, 12450–12453.
20 P. Chambon, A. Blanazs, G. Battaglia and S. P. Armes, *Macromolecules*, 2012, **45**, 5081–5090.
21 Q. Qu, G. Liu, X. Lv, B. Zhang and Z. An, *ACS Macro Lett.*, 2016, **5**, 316–320.
22 C. A. Figg, A. Simula, K. A. Gebre, B. S. Tucker, D. M. Haddleton and B. S. Sumerlin, *Chem. Sci.*, 2015, **6**, 1230–1236.
23 W. Zhou, Q. Qu, W. Yu and Z. An, *ACS Macro Lett.*, 2014, **3**, 1220–1224.
24 L. Qiu, C. R. Xu, F. Zhong, C. Y. Hong and C. Y. Pan, *Macromol. Chem. Phys.*, 2016, **217**, 1047–1056.
25 J. Huang, H. Zhu, H. Liang and J. Lu, *Polym. Chem.*, 2016, **7**, 4761–4770.
26 J. B. Tan, D. D. Liu, C. D. Huang, X. L. Li, J. He, Q. Xu and L. Zhang, *Macromol. Rapid Commun.*, 2017, **38**, 1700195.
27 M. Chen, J. W. Li, W. J. Zhang, C. Y. Hong and C. Y. Pan, *Macromolecules*, 2019, **52**, 1140–1149.
28 J. Z. Du and R. K. O'Reilly, *Soft Matter*, 2009, **5**, 3544–3561.
29 H. Deng, J. Liu, X. Zhao, Y. Zhang, J. Liu, S. Xu, L. Deng, A. Dong and J. Zhang, *Biomacromolecules*, 2014, **15**, 4281–4292.
30 W. W. Gao, J. M. Chan and O. C. Farokhzad, *Mol. Pharm.*, 2010, **7**, 1913–1920.
31 S. Binauld and M. H. Stenzel, *Chem. Commun.*, 2013, **49**, 2082–2102.
32 H. Wei, R. X. Zhuo and X. Z. Zhang, *Prog. Polym. Sci.*, 2013, **38**, 503–535.
33 N. Kamaly, B. Yameen, J. Wu and O. C. Farokhzad, *Chem. Rev.*, 2016, **116**, 2602–2663.
34 W. J. Zhang, C. Y. Hong and C. Y. Pan, *ACS Appl. Mater. Interfaces*, 2017, **9**, 15086–15095.
35 H. Wei, L. R. Volpatti, D. L. Sellers, D. O. Maris, I. W. Andrews, A. S. Hemphill, L. W. Chan, D. S. H. Chu, P. J. Horner and S. H. Pun, *Angew. Chem., Int. Ed.*, 2013, **52**, 5377–5381.
36 J. Tan, L. Fu, X. Zhang, Y. Bai and L. Zhang, *J. Mater. Sci.*, 2016, **51**, 9455–9471.
37 G. P. Lokhande and R. N. Jagtap, *Prog. Org. Coat.*, 2016, **90**, 359–369.
38 H. Zhu, Q. C. Liu and Y. M. Chen, *Langmuir*, 2007, **23**, 790–794.
39 J. Cao, L. F. Zhang, X. Q. Pan, Z. P. Cheng and X. L. Zhu, *Chin. J. Chem.*, 2012, **30**, 2138–2144.
40 K. Knop, R. Hoogenboom, D. Fischer and U. S. Schubert, *Angew. Chem., Int. Ed.*, 2010, **49**, 6288–6308.
41 S. N. S. Alconcel, A. S. Baas and H. D. Maynard, *Polym. Chem.*, 2011, **2**, 1442–1448.
42 R. Duncan, *Nat. Rev. Drug Discovery*, 2003, **2**, 347–360.
43 X. F. Xu, C. Y. Pan, W. J. Zhang and C. Y. Hong, *Macromolecules*, 2019, **52**, 1965–1975.
44 J. Z. Du, Y. Q. Tang, A. L. Lewis and S. P. Armes, *J. Am. Chem. Soc.*, 2005, **127**, 17982–17983.
45 A. Jager, E. Jager, F. Surman, A. Hocherl, B. Angelov, K. Ulbrich, M. Drechsler, V. M. Garamus, C. Rodriguez-Emmenegger, F. Nallet and P. Stepanek, *Polym. Chem.*, 2015, **6**, 4946–4954.
46 X. Zhang, J. Rieger and B. Charleux, *Polym. Chem.*, 2012, **3**, 1502–1509.
47 S. L. Canning, G. N. Smith and S. P. Armes, *Macromolecules*, 2016, **49**, 1985–2001.
48 E. R. Jones, M. Semsarilar, P. Wyman, M. Boerakker and S. P. Armes, *Polym. Chem.*, 2016, **7**, 851–859.
49 W. J. Zhang, C. Y. Hong and C. Y. Pan, *RSC Adv.*, 2015, **5**, 42637–42644.
50 W. J. Zhang, C. Y. Hong and C. Y. Pan, *Macromol. Rapid Commun.*, 2015, **36**, 1428–1436.
51 A. B. Lowe, *Polymer*, 2016, **106**, 161–181.
52 Y. W. Pei, A. B. Lowe and P. J. Roth, *Macromol. Rapid Commun.*, 2017, **38**, 1600528.